Tracking Control of a Conveyor Belt: Design and Experiments

M. C. Tsai and C. H. Lee

Abstract—**This paper presents the results of an experimental setup for a position tracking system that is to control a working table to track a workpiece on a moving conveyor belt, such that the manipulator placed on the working table is able to operate upon the workpiece while the workpiece is still moving. The feedback control employs a reflective-type optical sensor which is placed on the table, to measure the relative positions of the working table and the workpiece. A predictive method to compensate for the effect of sensor output saturation on tracking performance is investigated in detail. The application of this tracking control to industrial production lines to achieve a nonstop work flow may shorten overall manufacturing time, and therefore improve the production efficiency and increase the productivity.**

I. Introduction

In conventional manufacturing assembly lines, workpieces are transported to various workstations by the conveyor belt, and are often required to be disengaged from the moving conveyor at each workstation for processing. As shown in Fig. 1, when the workpiece arrives at the workstation, it is removed from the conveyor by a positioning mechanism, and then put back for transport to the next workstations after the required processing has been completed by the processing mechanism beside the conveyor. In this way, the processing mechanism is permanently fixed beside the conveyor. The whole process costs time not only during processing, but also during removal, positioning, and returning of the workpiece. In addition, transportation of the workpiece from one station to the next also adds more time to the process, in effect lengthening the entire manufacturing time and hence decreasing the average efficiency of the production. This explains the need to decrease the removal, processing, and returning time of the workpiece in order to maximize processing/manufacturing efficiency.

To combat the hindrances to high productivity mentioned above, this paper presents a position tracking control system that essentially consists of a moving conveyor and a working table (equipped with a processing mechanism) which is driven by a servo motor. On the table there is an optical sensor for position feedback control. As the working table tracks the workpiece, the processing mechanism is able to perform its task (such as assembly, detection, inspection, etc.) on the moving workpiece on-line without the need to stop the workpiece at each workstation. A specific feature of this kind of processing in production lines is that of accomplishing the task in the way of simultaneously transporting and processing the workpiece. Using the concept of *tracking and working*, not only could the time of positioning and/or removal of workpieces be spared, but also the manufacture flow could be maintained continuously. Thus the savings in the process time would increase the productivity in production lines.

This paper is organized as follows. First, the overall scheme of the proposed tracking system is explained and the inherent nonlinearity of the reflective-type feedback sensor is examined. Then the H^{∞} loop shaping method of [5] and [6] is employed to design a robust position controller, and a predictive method to compensate for the sensor output saturation is also provided for improving tracking performance. Finally, experimental results are given to evaluate the effectiveness of our proposed control method.

Manuscript received September 24, 1993; revised November 3, 1994. This work was supported by the National Science Council of the Republic of China under Contract NSC 82-0422-E-006-051.

The authors are with the Department of Mechanical Engineering, National Cheng Kung University, Tainan, Taiwan 701 R.O.C.

Publisher Item Identifier S 1042-296X(96)00489-7.

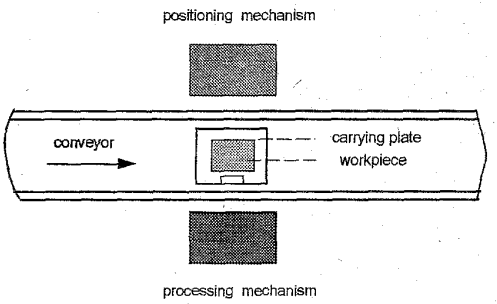

Fig. 1. The schematic diagram of a traditional manufacturing flow line.

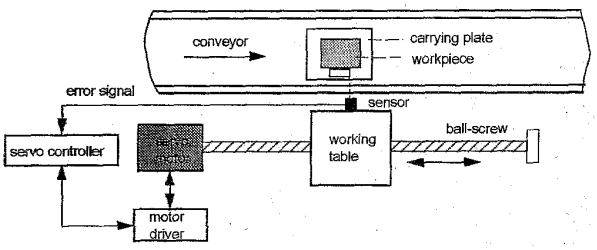

Fig. 2. The schematic diagram of a position tracking system.

II. A Position Tracking System

The schematic diagram of the proposed tracking system for improving production efficiency is shown in Fig. 2. The system consists of a servo motor, a motor driver, a lead ball-screw, a working table, a servo controller, a photoelectric sensor, and a conveyor belt. The working table moves parallel to the conveyor flow line and is controlled by the servo controller via a reflective optical sensor, allowing the table to track the moving workpiece. Fig. 3 is the block diagram of the closed-loop control system. The working table is initially at a home position waiting for an arriving workpiece. When a product is sensed, the servo controller calculates a correct distance, and adjusts the motion of the working table to track the workpiece correctly with respect to the carrying plate. Once the speeds of the workpiece and the working table are synchronized, the processing mechanism mounted on the working table begins the implementation of the desired tasks on the assembly line. From the point of view of an observer sitting on the working table, the workpiece under processing looks stationary. After the processing is complete, the working table quickly returns to the home position and then waits for the next carrying plate to repeat the process.

The optical sensor used in our setup for synchronizing control is an analog output type photoelectric switch, the OMRON type E3SA [10]. This is a reflective sensor, often used for mark detection in production lines as an on/off switch, which is here used to sense the leading edge of the incoming carrying plate on the conveyor. Thus the tracking system of Fig. 2 is in no way coupled to the conveyor, making it useful for many applications. We now examine the characteristics of

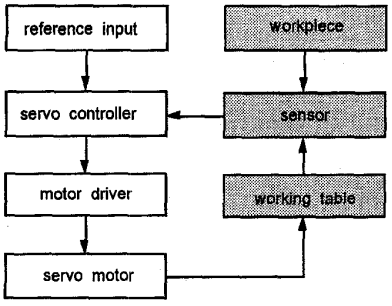

Fig. 3. The block diagram of the tracking control system.

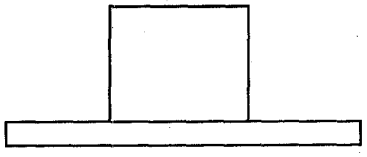

Fig. 4. Carrying plate (front view).

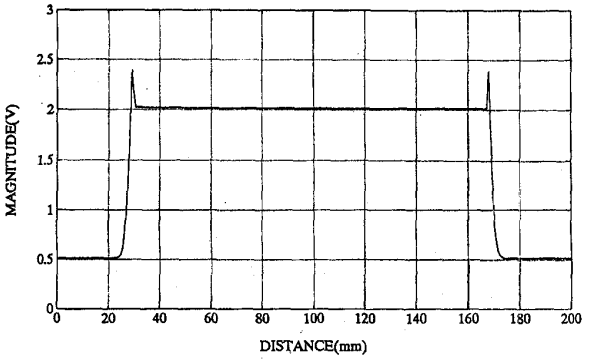

Fig. 5. Characteristics of the optical sensor: voltage versus displacement.

the feedback sensor. Let the sensor scan the face of the carrying plate of Fig. 4. We obtain a plot of voltage versus displacement as shown in Fig. 5. As can be seen, there is a steep linear region (i.e., the region **L** about 3 mm long on the "x-axis") when the sensor passes the edge of the face. Taking the average "y-value" of the linear portion as an input reference value, the aim of the servo controller is to keep the error between the measured signal and the reference input as small as possible. The error value is proportional to the displacement error by the slope of the linear range in Fig. 5; keeping the error small will keep the working table and the moving workpiece in synchronized motion. Thus the processing mechanism (e.g., a robot manipulator) on the working table is able to work on the workpiece without the need to stop the conveyor. Clearly the use of the tracking system will save much of the idle time spent by the conventional manufacturing assembly line, since here the processing mechanism performs its task directly on the moving workpiece, and quickly returns to its home position for the next workpiece.

III. Robust Controller Design

Feedback control design using the H^∞ theory [1] has been well developed in recent years. The H^∞ control design can easily combine several specifications such as disturbance attenuation, asymptotic tracking, bandwidth limitation, and robust stability into a single minimax frequency domain control problem. One of the well-known

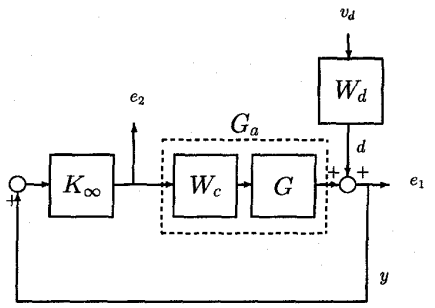

Fig. 6. A weighted mixed sensitivity design problem.

methods in feedback design is called *loop shaping* [8], in that the closed-loop objectives are specified in terms of open-loop singular values of the compensated system. A loop shaping design procedure using H^∞ synthesis was introduced by McFarlane and Glover [6], who incorporate the loop shaping to obtain a performance/robust stability trade-off. The design procedure consists of two main stages.

1) Shape the original system using a precompensator and/or a postcompensator, to give a desired open-loop shape.
2) Apply H^∞ control, based on the normalized coprime factorization problem, to find a robust stabilizer for this shaped plant.

In contrast to the classical loop shaping approach, the H^∞ loop shaping design procedure is done *without* explicit regard for the original plant phase information. That is, closed-loop stability requirements are disregarded at this stage. Also, the robust stabilization is achieved *without* frequency weight. The result is that the designer can easily specify the closed-loop objectives in terms of open-loop singular values using the classical control techniques. In the following, we introduce briefly the H^∞ loop shaping design procedure of [5] and [6] which is used to design the position controller of our tracking system.

Consider the weighted mixed sensitivity design problem depicted in Fig. 6 where the plant G is to be controlled by compensator $K(=W_cK_\infty)$. Disturbances to the system are represented by an equivalent disturbance d at the plant output. The function of K_∞ is to stabilize the shaped plant $G_a = GW_c$ where W_c is a shaping function, typically chosen as a low-pass filter with a desired frequency roll-off rate [7] in order to mitigate the effects of high-frequency noise. Consequently, good disturbance attenuation, robustness, limited bandwidth and compensator roll-off may be obtained by finding a stabilizing controller K_∞ which minimizes the cost function

$$\left\| \begin{bmatrix} S \\ K_\infty S \end{bmatrix} W_d \right\|_\infty \tag{1}$$

where $S = (I - G_aK_\infty)^{-1} = (I - GK)^{-1}$, $W_d = \tilde{M}^{-1}$ and $\tilde{M}$ is the denominator of the left coprime factorization of $G_a(=\tilde{M}^{-1}\tilde{N})$ satisfying

$$\tilde{N}(s)\tilde{N}^T(-s) + \tilde{M}(s)\tilde{M}^T(-s) = I.$$

Such a design problem has been shown, for example in [4] and [9], to be very useful in practice, and of course it obviates the need for γ-iteration in computing the optimal solution.

As with any control system design methodology, design process is iterative. A summary of the loop shaping design procedure is given below.

1) Select a shaping function W_c such that the shaped plant $G_a = GW_c$ meets certain specifications, i.e., a desired open-loop shape.

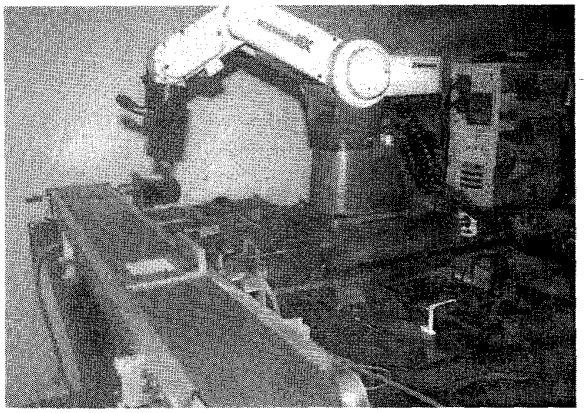

Fig. 7. An experimental set up for synchronous tracking/working.

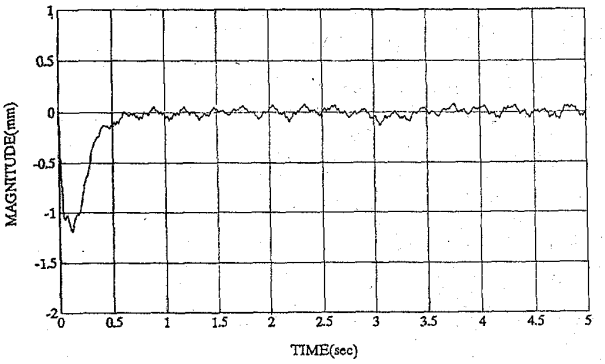

Fig. 8. A tracking error plot at the conveyor speed = 4.68 cm/s.

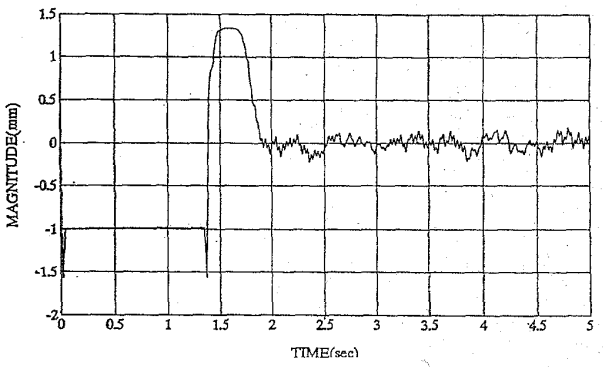

Fig. 9. A tracking error plot at the conveyor speed = 13.26 cm/s.

2) Compute the normalized coprime factorization of $G_a = \tilde{M}^{-1}\tilde{N}$, which requires the solving of an algebraic Riccati equation.
3) Find an optimal H^∞ controller K_∞ to minimize the cost of (1).
4) Form the final controller $K = W_c K_\infty$, and then evaluate the closed-loop performances by computer simulations. If the closed-loop system fails to meet design specifications, go to the first step.

Our experimental setup for the tracking system is shown in Fig. 7, where the processing mechanism on the working table is a robot manipulator. It should be noted that since the working table and workpiece are stationary relative to each other, a wide variety of tasks might be performed which would otherwise be very difficult if the robot itself were also responsible for tracking (also see Remark 1 below). The working table is driven by a ball screw (1 mm/rev), which is connected to a SANYO BL865 AC servo motor (100 W). The transfer function of the controlled plant of Fig. 7 was found by using an HP3563A control system analyzer to measure the frequency responses. This gives a nominal model, $G(s)$, of the controlled plant as

$$G(s) = \frac{1\,021\,600\,000}{s(s^2 + 72.3s + 7481.9)}$$

for use in designing the controller. To achieve no steady state errors design, we choose the shaping weight W_c to be a PI-type, where

$$W_c = \frac{0.000\,125(s+8)}{s}.$$

Following the H^∞ loop shaping design procedure yields that the optimal cost of (1) is 1.5735 and the optimal controller is

$$K_\infty(s) = \frac{2s^3 + 121s^2 + 12\,158s + 52\,594}{s^3 + 116s^2 + 11\,493s + 82\,757}.$$

The final controller is then given by $K(s) = K_\infty(s)W_c(s)$.

Remark 1: The use of the robot manipulator is merely to demonstrate the possibilities of the tracking and working setup. In the controller design, it is assumed that forces between the robot and the workpiece are negligible. Indeed, in practice, robots used for inspection will encounter little or no loads, while those used for actual working will encounter varying loads.

The performance of the controller design in our setup is evaluated by a digital signal processor, the TMS320C30 DSP. The control algorithms are written in C-language and are all executed in the floating-point format. The outputs of the controller, $K(s)$, are sent to the servo motor drive, the input of the controlled plant, via a 16-b digital to analog converter. The relative positions of the working table and the workpiece received from the optical sensor are sent to the DSP via a 16-b analog to digital converter. To implement the continuous-time controller $K(s)$ on the DSP, we use the zero-order-hold of sampled-data systems to get a discrete-time controller. The reader is referred to [2] for a survey on implementation of digital controllers. In following experiments the sampling period is $h = 120\ \mu s$.

We now examine the tracking performance resulting from the above design. At the beginning, the sensor (on the working table) is waiting at the home position for the incoming workpiece. When the sensor detects the workpiece, it transmits a starting signal to the servo controller for tracking control. Because of different initial speeds of the conveyor and the table, tracking will display a temporary phenomenon of lagging behind as shown in Figs. 8 and 9. Fig. 8 shows a tracking error plot measured for the case in which the conveyor is moving at the speed of 4.68 cm/s. For such a low speed, the synchronizing only takes about 0.5 s. However, as the conveyor speed is increased to 13.26 cm/s, it takes 1.9 s for the synchronizing as shown in Fig. 9. These figures indicate that greater conveyor speed requires more time to achieve tracking control. Further, it can be found in [3] that the tracking performances are almost the same in the cases of the working table with and without the robot (about 20 kg in weight), respectively.

Observing Fig. 5, we see that the sensing signal is very sharp as the sensor passes the edge of the carrying plate. This is due to the exceptionally high reflective characteristic of the sharp edges. However, as can also be seen from Fig. 5, the sensor signal appears to have the same value between the two edges because the carrying plate is essentially flat, giving off the same saturated reflection. The sensor output saturation causes the time taken to establish tracking control to be longer. To reduce the time of completing the tracking

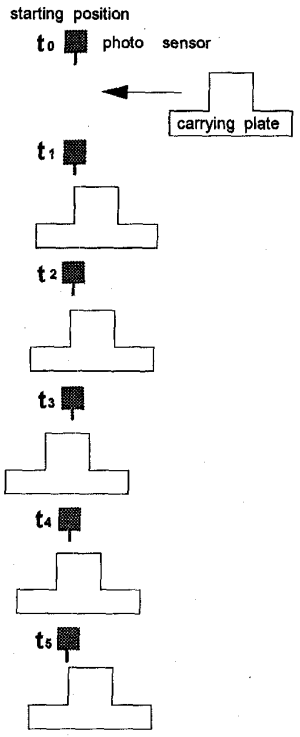

Fig. 10. The timing sequence of the tracking.

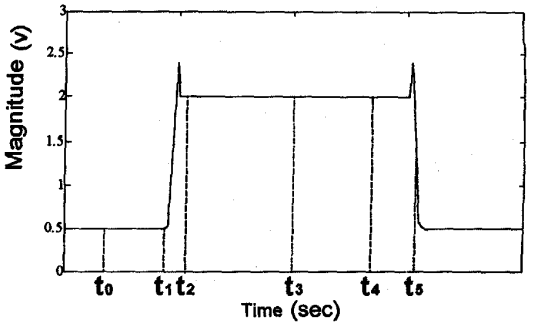

Fig. 11. The timing diagram of the sensor signal.

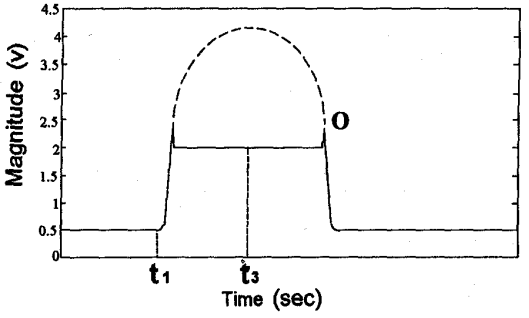

Fig. 12. The curve of a predicted sensor signal.

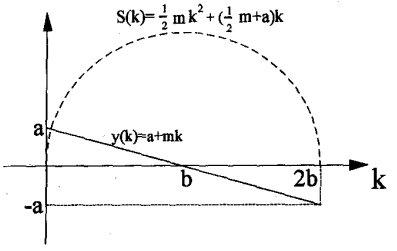

Fig. 13. The conceptual diagram of the compensation.

control at certain operating speeds, Section IV presents a predictive method to overcome the effect of the sensor output saturation in that the position controller is assumed to be given and also fixed.

IV. A Method to Compensate for the Saturation

The timing sequence of the tracking process is shown in Fig. 10. At time t_0, the sensor is waiting at the home position. At time t_1, the workpiece comes into the tracking region and begins to be tracked. Then at time t_2, the sensor is in the region of saturation. The largest tracking error occurs at the time t_3. As time passes, tracking error dwindles, as seen at time t_4, and complete tracking control is established at time t_5. Fig. 11 shows the sensed signal with respect to the timing of Fig. 10. As time passes from t_2 to t_3, the sensed error signal remains unchanged, because of the saturation of the sensor, but actual error continues to increase. This saturated behavior will clearly affect the tracking performance because the sensed error signal cannot respond to different tracking errors. It should be noted that the controller and the carrying plate are designed such that the sensor cannot bypass the trailing edge of the carrying plate, i.e. the carrying plate is sufficiently wide.

One method to overcome the saturated signal is to generate error signals in accordance with actual tracking errors as shown in Fig. 12, where the dashed line represents a predicted signal while the solid line is the measured sensor signal. The basic technique of the predictive method is explained in the following.

Let the linear curve (the solid line) of Fig. 13 be given by

$$y(k) = a + mk \tag{2}$$

where $m = -a/b$ is the slope of the curve, and the integer k denotes a discrete-time function with the unit being the sampling period h. Integrating (2) will yield a second differentiable parabola (i.e., the dashed line of Fig. 13) given by

$$\begin{aligned} S(k) &= y(1) + y(2) + y(3) + \cdots + y(k) \\ &= (a+m) + (a+2m) + (a+3m) + \cdots + (a+km) \\ &= \frac{1}{2}mk^2 + \left(\frac{1}{2}m + a\right)k. \end{aligned} \tag{3}$$

In fact, we have

$$y(k) = y(k-1) + m,\ y(0) = a \tag{4}$$

and

$$S(k) = S(k-1) + y(k),\ S(0) = 0. \tag{5}$$

The recursive forms are instrumental in the real-time calculation.

The parabolic curve defined in (5) is a function of a and b, so they can be properly chosen prior to use of the predicted feedback signal to improve tracking performance, i.e., by reducing the *settling time* of the tracking control. Note that the time period taken to achieve a tracking error margin of ± 0.2 mm is hereafter called the *settling time*. Our experiments have shown that the values of a and/or b are required to increase relative to the increase in conveyor speed.

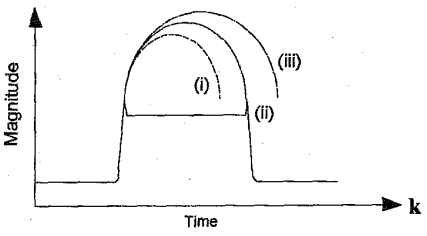

Fig. 14. Three possible outcomes from using the predicted signal.

Remark 2: The conveyor's average speed is assumed to be constant. However, instantaneous velocity may vary slightly, making it difficult to specify beforehand the steady-state tracking precision requirements. The ± 0.2 mm we observed is certainly satisfactory for many applications. Our primary goal, however, is to decrease the settling time. Since settling time is a function of the desired precision, increasing precision will also increase settling time. This trade-off would need to be dealt with on a case-by-case basis.

The control principle with the predicted signal is as follows. When the measured sensor signal is greater than a preset value which represents the time in the saturated region, the control system switches to using the predicted signal given by the dashed curve of Fig. 12, (computed from (4) and (5)). After counting $2b$ times, the control system returns to using the measured sensor signal automatically. The ideal result of using this method is that the return after $2b$ times is exactly on point **O** of Fig. 12. However, in practice, this may not always be the case. In general, as shown in Fig. 14, there are three possible situations:

i) the predicted value is too small;
ii) compensation is perfect; and
iii) the predicted value is too large.

To improve Case i) (or Case iii)) is to increase (or decrease) the parameters a and/or b accordingly. The "optimal" a and/or b which result in Case ii), can be found by experiments from an iterative tuning process. As will be seen in the next section, the predictive method can effectively overcome the problem due to the sensor output saturation, hence it has the benefit of having a much shorter time $\tilde{t}_3$ (see Fig. 12) than the original time t_3 (see Fig. 11), thus being able to minimize the settling time of the tracking control.

V. Experimental Results

In this section, under the condition that the position controller is fixed, we examine tracking performance without and with the predictive method. In the case of the conveyor running at the speed of $v = 9.43$ cm/s, the dashed line of Fig. 15 shows that the settling time of the tracking system without any care on the feedback signals is 1.30 s. Using the predictive method with $b = 1000$, the "optimal" $a = 15.0$ such that the system response is of Case ii) was found, iteratively, from several experiments. In this case, the settling time is 0.5 s (see the solid line of Fig. 15). Fig. 16 shows the experimental results for $v = 15.58$ cm/s. Here, the improvement by the predictive method becomes more evident as the speed of the conveyor becomes faster. Table I summarizes some experimental data from five different speed settings where T_1 and T_2 are the settling times in both cases of without and with sensor compensation, respectively. An asterisk $(*)$ signifies that the tracking control fails.

As can be seen from Table I, the faster the speed of the conveyor, the larger the value of a required, thus the parameter a should be tuned properly with respect to the conveyor speed. Our experiments conclude that using the predictive method the settling time of the tracking control can be effectively reduced. From experimental results

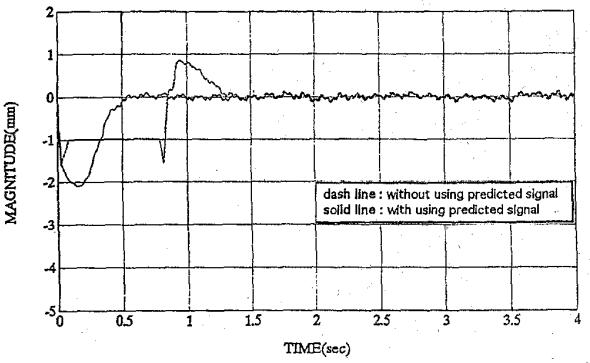

Fig. 15. The tracking error plot for $v = 9.43$ cm/s.

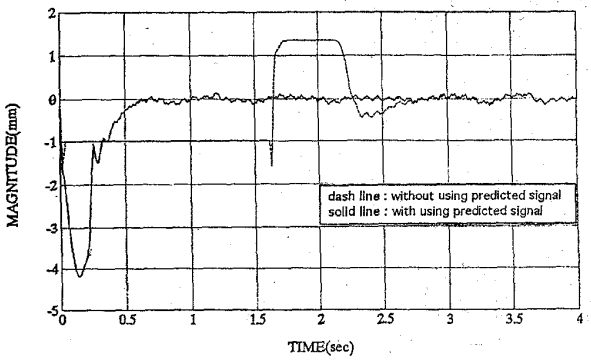

Fig. 16. The tracking error plot for $v = 15.58$ cm/s.

TABLE I
The Relations Between a and Conveyor Speed

	Conveyor speed (cm/sec)	a	$T_1(sec)$	$T_2(sec)$
# 1	9.43	15.0	1.30	0.50
# 2	13.26	35.0	1.90	0.50
# 3	17.99	55.0	3.10	0.57
# 4	22.22	75.0	*	0.62
# 5	26.60	95.0	*	0.65

shown in Table I, we found that the "optimal" parameter a is a function of the conveyor speed, v. Using the least-squares fit, a linear curve was found as

$$a(v) = 4.5907v - 27.0912 \tag{6}$$

where the speed of the conveyor (v) is measurable. As the conveyor speed is known, this relationship provides a good estimated a for the predictive method to reduce the settling time of our proposed tracking system. Now we arbitrarily set two different conveyor speeds to verify the validity of using (6). Letting $v_1 = 15.02$ cm/s and $v_2 = 23.04$ cm/s, we obtain $a(v_1) = 41.9$ and $a(v_2) = 78.7$. The settling time of the tracking control without and with modification of the sensor output are $T_1 = 2.5$ s and $T_2 = 0.55$ s, respectively, at the speed of $v = v_1$. For the speed of $v = v_2$, the tracking control fails due to sensor output saturation, but the settling time of the tracking control using the predictive method only takes $T_2 = 0.62$ s. Note that we here maintain b as constant; the same can also be done keeping a constant and varying b.

The experimental results presented above have shown that the predictive method by using (2) with $b = 1000$ (a fixed constant) and a

given by (6) can successfully shorten the settling time of the tracking control at different operation speeds. In our experimental setup the settling time is in the range of $0.50 \sim 0.65$ s for the conveyor belt running between $9.43 \sim 26.60$ cm/s. As we have seen, this is a great improvement in the tracking control compared with that where no special care is taken to compensate for the feedback signal when the sensor is operating in the saturated region. Again, the advantage of the predictive method becomes more evident as the speed of the conveyor becomes faster.

VI. Conclusion

This paper presents a position tracking control for use in production lines. The concept of synchronous tracking and working is of great industrial applicability, and has positive effects on shortening manufacturing time and increasing manufacturing efficiency. An H^∞ robust controller has been implemented successfully in an experimental setup with a robot arm sitting on the working table. The design problem of sensor output saturation was successfully dealt with by using a predictive method while the sensor is operating in the saturated range.

In our experiments only one processing mechanism was used at a time. It might be possible, however, to use two or more simultaneously tracking and working devices in conjunction, and thereby further increase productivity.

References

[1] B. A. Francis, *A Course in H^∞ Control Theory*. Berlin: Springer-Verlag, 1987.

[2] H. Hanselmann, "Implementation of digital controllers—A survey," *Automatica*, vol. 23, pp. 7–32, 1987.

[3] C. H. Lee, "Performance improvement of a synchronous tracking control system," Master's thesis, National Cheng Kung University, Tainan, Taiwan, 1993.

[4] R. A. Hyde and K. Glover, "A comparison of different scheduling techniques for H^∞ controllers," *Trans. Inst. Meas. Contr.*, vol. 13, pp. 227–232, 1991.

[5] D. McFarlane and K. Glover, "A loop shaping design procedure using H^∞ synthesis," *IEEE Trans. Automat. Contr.*, vol. 37, pp. 759–769, 1992.

[6] ——, *Robust Controller Design Using Normalized Coprime Factor Plant Descriptions*. Berlin: Springer-Verlag, 1990.

[7] I. Postlethwaite, M. C. Tsai, and D. W. Gu "Weighting function selection in H^∞ design," in *Proc. IFAC Conf.*, Tallinn, Estonia, 1990, vol. 3, pp. 127–132.

[8] M. G. Safonov, A. J. Laub, and G. L. Hartmann, "Feedback properties of multivariable systems: The role and use of the return difference matrix," *IEEE Trans. Automat. Contr.*, vol. AC-26, pp. 47–65, 1981.

[9] D. J. Walker and I. Postlethwaite, "Discrete time H^∞ control laws for a high performance helicopter," in *Proc. 30th IEEE Conf. Decision and Control*, Brighton, England, 1991, vol. 1, pp. 128–129.

[10] OMRON Inc., *The OMRON Handbook: Best Control Machines*, 11th ed., Japan, 1992.

Approximate Inverse Dynamics and Passive Feedback for Flexible Manipulators with Large Payloads

Christopher J. Damaren

***Abstract*— A derivation is presented of an approximate form of the dynamics governing a structurally flexible manipulator carrying a massive payload at its end-effector. An output called the μ-tip rate which incorporates end-effector and elastic motions is introduced. The input-output mapping relating a transformed version of the joint torques to the μ-tip rates is shown to be passive for large payloads. A feedforward torque strategy is developed which preserves the passivity property in the error dynamics and a suitable Lyapunov function is used to demonstrate global asymptotic stability of the tracking provided by a PD law. Implementation of the controllers without measurements of the elastic coordinates and rates is shown to be possible. Simulation studies of a six DOF manipulator with flexible links, modeled after the Shuttle Remote Manipulator System, demonstrate excellent tracking in all six Cartesian end-effector coordinates, even for payloads with modest mass properties. A major conclusion is that some of the problems normally associated with lack of collocation in flexible manipulators can be surmounted when large (massive) payloads are involved.**

I. Introduction

In the last two decades, a coherent theory of control for rigid robot manipulators has emerged. Globally stable trajectory tracking has been demonstrated with respect to "exact" nonlinear models of rigid robot dynamics. The tutorial paper [1], while primarily focusing on adaptive control, presents a useful subdivision of globally stabilizing controllers into those based on feedback linearization and those which exploit the concept of passivity. The success of controllers in the latter group can be attributed to the collocation of torque actuation and joint rate sensing which ensures passivity in the open-loop forward dynamics operator [2].

General mechanical systems possessing collocation of force inputs and rate outputs such as flexible space structures [3] exhibit passivity on account of the energy balance between the system Hamiltonian and the work done by inputs and dissipative influences. The major importance of this concept in controller synthesis arises from the Passivity Theorem (see [4] for example) which states that the feedback interconnection of a passive system and a strictly passive one is input-output stable. The recognition that passive systems possess a natural Lyapunov function in the form of the storage function [5], [6] leads to the more common notion of Lyapunov stability. For passive mechanical systems, the storage function can usually be identified with the Hamiltonian which has been fully exploited in controlling rigid manipulators. In the case of structurally flexible manipulators, the passivity of the map relating the applied torques to the joint rates persists given the physical collocation. However, this knowledge is less strategic than in the rigid case since the true goal is usually tracking of a prescribed end-effector trajectory.

In general, the map from joint torques to end-effector rates is not passive for a flexible arm. In the case of a single flexible link, it is well-known that the transfer function from joint torque to tip rate is nonminimum phase. As noted in [7], the forward dynamics operator in the multilink case exhibits the nonlinear analog of the nonminimum phase property in linear systems, namely instability

Manuscript received February 11, 1994; revised January 1, 1995.

The author is with the Department of Mechanical Engineering, University of Canterbury, Christchurch, New Zealand.

Publisher Item Identifier S 1042-296X(96)01066-4.